Journal of Geriatric Cardiology JGC
RESEARCH ARTICLE
J Geriatr Cardiol 2023; 20(5): 341–349

Identification of an *LDLR* variant in a Chinese familial hypercholesterolemia and its relation to ROS/NLRP3-Mediated pyroptosis in hepatic cells

Wen-Zhuo CHENG[1,*], Wei-Hua WANG[2,*], Ai-Ping DENG[3], Xiao DANG[4], Chao LIU[5], Xian-Can WANG[6,✉], Ju-Yi LI[3,✉], Si JIN[1,✉]

1. Department of Endocrinology, Institute of Geriatric Medicine, Liyuan Hospital, Tongji Medical College, Huazhong University of Science and Technology, Wuhan, Hubei, China; 2. Department of Party Affairs, Pulmonary and Critical Care Medicine, The Central Hospital of Wuhan, Tongji Medical College, Huazhong University of Science and Technology, Wuhan, Hubei, China; 3. Department of Pharmacy, Central Hospital of Wuhan, Tongji Medical College, Huazhong University of Science and Technology, Wuhan, Hubei, China; 4. Department of Prenatal Diagnostic Center, Guangzhou Women and Children's Medical Center, Guangzhou Medical University, Guangdong, China; 5. Hubei Key Laboratory of Diabetes and Angiopathy, Hubei University of Science and Technology, Wuhan, Hubei, China; 6. Department of Cardiovascular Surgery, Central Hospital of Wuhan, Tongji Medical College, Huazhong University of Science and Technology, Wuhan, Hubei, China

[*]The authors contributed equally to this manuscript

✉ Correspondence to: dr_can@126.com (WANG XC); ljywxf110@163.com (LI JY); jinsi@hust.edu.cn (JIN S)

https://doi.org/10.26599/1671-5411.2023.05.003

ABSTRACT

BACKGROUND Familial hypercholesterolemia (FH) is a common autosomal dominant hereditary disease. Its early diagnosis and intervention significantly improve the patient's quality of life. However, there are few types of research on the FH pathogenic genes in China.

METHODS In this study, we recruited a family diagnosed with FH and used whole exome sequencing (WES) to analyze the proband variants. Intracellular cholesterol level, reactive oxygen species (ROS) level, and the expression of pyroptosis-related genes were detected after overexpression of wild-type or variant *LDLR* in L02 cells.

RESULTS A heterozygous missense variant predicted to be deleterious to *LDLR* (c.1879G > A, p.Ala627Thr) was identified in the proband. Mechanistically, intracellular cholesterol level, ROS level, and the expression of pyroptosis-related genes, nucleotide-binding oligomerization domain-like receptor family protein 3 (NLRP3) inflammasome and components (caspase 1, apoptosis-associated speck-like protein containing a caspase recruitment domain (ASC) and NLRP3), gasdermin D (GSDMD), interleukin (IL) -18, IL-1β was elevated in the variant *LDLR* group, which was attenuated by inhibition of ROS.

CONCLUSIONS FH is associated with a variant (c.1879G>A, p.Ala627Thr) in the *LDLR* gene. Regarding the mechanism, the ROS/NLRP3-mediated pyroptosis in hepatic cells may contribute to the pathogenesis of the *LDLR* variant.

Familial hypercholesterolemia (FH; MIM# 143890) is an autosomal dominant genetic disease, and the incidence of FH is about 1 in every 500 worldwide,[1] which is mainly caused by pathogenic variants of low-density lipoprotein receptor (LDLR), apolipoprotein B (apo B), or proprotein convertase subtilisin-Kexin type 9 (PCSK9) encoding genes.[2,3] Moreover, it is also caused by variants in *LDLRAP1*,[4,5] *STAP1*, *APOE*, and *LIPA* genes.[6–8] In addition, people with hypercholesterolemia may not necessarily have genetic abnormalities.

The clinical manifestations of FH include skin and tendon xanthomas, corneal arcus, and premature symptoms of coronary artery disease. FH is characterized by high plasma LDL and cholesterol

levels, which are also risk factors for atherosclerosis.[9] With the recent development of sequencing technology, whole-exome sequencing (WES) is gradually being embraced in clinical settings to identify the changes in all functional gene sequences in diabetes, prenatal genetics, and other fields.[10–12] In some European countries, the use of second-generation sequencing to diagnose FH has become very popular. However, its diagnosis rate in China is less than 1%,[13] mainly because it solely depends on clinical manifestations and family history. In addition, it is possible to ignore FH patients because not all of them exhibit obvious clinical indications. The FH variant spectrum in China remains to be further elucidated.

It was well known that the liver uptakes LDL particles via LDLR [14,15] and LDL is the major cholesterol-carrying lipoprotein in humans.[16] Intracellular cholesterol crystals have been shown to induce NLRP3 inflammasome activation,[17] which was associated with pyroptosis.[18,19] However, whether the NLRP3 inflammasome assembly primes hepatic cells and mediates their pyroptosis remains unknown after the *LDLR* variant.

By using WES and Sanger sequencing, we reported a variant in the *LDLR* (c.1879G > A, p.Ala627Thr) in one Chinese family with FH. Our data showed that this variant may be associated with ROS/NLRP3-mediated pyroptosis. The aim of this research is to screen out FH-related variants by utilizing WES technology and further expand the FH variant spectrum in China, and we anticipate that the mechanism study can contribute to better combinations in future FH therapy.

METHODS

Patient Enrollment

Written informed consent of participation and publication of any potentially identifiable images or data was obtained from all the participants in this study. Families with FH patients in the Central Hospital of Wuhan fulfilling the diagnostic criteria of Simon Broome Familial Hypercholesterolemia Register [20] were recruited. Patients with hypercholesterolemia due to other causes were excluded.

Clinical and Laboratory Assessment

The specific family with FH was recruited by assessing the proband's (II-2) clinical manifestations and reviewing the family history. Next, the serum triglyceride (TG), total cholesterol (TC), high-density lipoprotein cholesterol (HDL-C), low-density lipoprotein cholesterol (LDL-C), apolipoprotein A (apo A), and apo B were determined in all subjects after fasting for at least 12 h.

DNA Extraction and Whole-exome Sequencing

Genomic DNA was extracted from the peripheral blood drawn from all the subjects using a commercial DNA extraction kit (TIANGEN, Beijing, China) following the manufacturer's procedure. Next, the obtained DNA was prepared for next-generation sequencing using a commercial kit (SureSelect Human All Exon V5, Agilent) following the manufacturer's protocol. Finally, exome sequencing was performed on the Illumina HiSeq2500 system.

Sequence Analysis

The sequenced paired reads were mapped to the NCBI Build 37 (hg19) reference genome. Next, SNVs and Indels were analyzed using public databases ExAC, dbSNP, ESP, and 1,000 genomes prioritizing variant genes related to FH published in PubMed. Non-exonic and synonymous variants were excluded; thus, only variants associated with FH were analyzed. In addition, in-silico prediction tools including SIFT, PolyPhen2, Variant Taster, Variant Assessor, FATHMM, and GERP plus were used to evaluate the relation of the predicted pathogenic variants to the diseases.[21–23]

Sanger Sequencing

The predicted pathogenic variants were further verified by Sanger sequencing.

Structure Modeling

The three-dimensional (3D) structure of the protein with a missense variant was simulated using the Swiss-Prot repository (http://web.expasy.org/docs/swiss-prot_guideline.html).

Reagents

DiI-LDL was purchased from Yiyuan (Guangzhou, China). ROS assay kit (S0033S) was purchased from Beyotime (Beijing, China). N-acetyl-L-cysteine (NAC) (HY-134495) were purchased from MedChemEx-

press (Shanghai, China). Annexin V-PE/7-AAD detection kit (A211) was purchased from Vazyme (Nanjing, China) Total Cholesterol（TC）Content Assay Kit (E1015) was purchased from Applygen (Beijing, China).

Cell Culture

L02 cells was cultured in DMEM (SH30022.01, HyClone, USA) supplemented with 10% foetal bovine serum (2500, ScienCell, Carlsbad, CA, USA) and 1% penicillin streptomycin (0503, ScienCell, Carlsbad, CA) at 37 °C in a humidified atmosphere of 5% CO_2.

Plasmid Transfection

Vector plasmids (pcDNA3.1) and plasmids overexpressing wild type or variant *LDLR* were synthesized by Genecreate (Wuhan, China). L02 cells were seeded and transfected with the indicated plasmids at a concentration of 2 μg for 48 h using an Effectene transfection reagent (Qiagen, Hilden, 301427) according to the manufacturer's guidelines.

Western Blot

Total protein (20 μg) in 10 μl supernatant was loaded onto an SDS–PAGE gel, separated, and immunoblotted using primary antibodies. Next, membranes were incubated with HRP-labelled goat anti-rabbit IgG (H+L) secondary antibody (1: 10,000; Abclone, Wuhan, China, A0208) for 1 h at room temperature, and immunoreactive bands were visualized by chemiluminescence (ECL assay). The following primary antibodies were used: anti-NLRP3 (1: 1000; Cell Signaling Technology, USA), anti-GSDMD (1: 1000; Abclonal, China), anti-ASC (1: 1000; Abclonal, China), anti-C-caspase-1 (1: 600; Cell Signaling Technology), anti-IL-18 (1: 1000; Abclonal, China), anti-IL-1β (1: 500; Cell Signaling Technology), and anti-β-actin (1: 4000; Proteintech, China). HRP goat anti-rabbit IgG (Abclonal, AS014) and HRP goat anti-mouse IgG (Abclonal, AS003) secondary antibodies were used at a 1: 10,000 dilution.

Confocal Imaging Analysis

L02 cells were incubated with DiI-LDL (200 μg/mL) for 24 h after vector plasmids (pcDNA3.1) and plasmids overexpressing wild type or variant *LDLR* transfection. Images were obtained using a confocal laser scanning microscope (FV3000, Olympus, Tokyo, Japan) using a 60× objective and analysed using ImageJ software (Santa Clara, CA, USA). For each sample, forty fields that included at least 15 cells were randomly selected, and the number of cells per field was counted. The fluorescence intensity was normalized to the number of cells per field.

Detection of Intracellular Cholesterol

Total intracellular cholesterol was measured according to the manufacturer's guidelines.

Detection of Reactive Oxygen Species (ROS)

ROS production in L02 cells were measured using microplate reader following the manufacturer's protocols.

Flow Cytometry Analysis

The integrity of cells was measured through Annexin V-PE/7-AAD dual fluorescent staining kit and quantified using flow cytometry. In line with the protocols above, 2×10^6 cells/well were seeded onto a 6-well plate and subjected to the indicated treatments. The cells were harvested and washed with PBS, from which 3×10^5 cells were separated and resuspended in 100 μL of binding buffer. Subsequently, 5 μL of Annexin V-PE and 5 μL of 7-AAD were added to the cells in order. After incubation at room temperature for 10 min in darkness, adding 400 μL binding buffer, the stained cells were placed on ice and subjected to the flow cytometry (Mindry, Bricyte E6).

Statistical Analyses

Data are expressed as the mean ± SE from at least three independent experiments. Multiple group comparisons were performed by one-way ANOVA followed by post hoc tests. Values with $P < 0.05$ were considered statistically significant.

RESULTS

Clinical Characteristics of Participants

The proband (II-2) was a 45-year-old man who was diagnosed with hypercholesterolemia at the age of 30 and had elbow induration at the age of 2. In addition, he has clinical manifestations of corneal arch (Figure 1A) and skin xanthomas (Figure 1B).

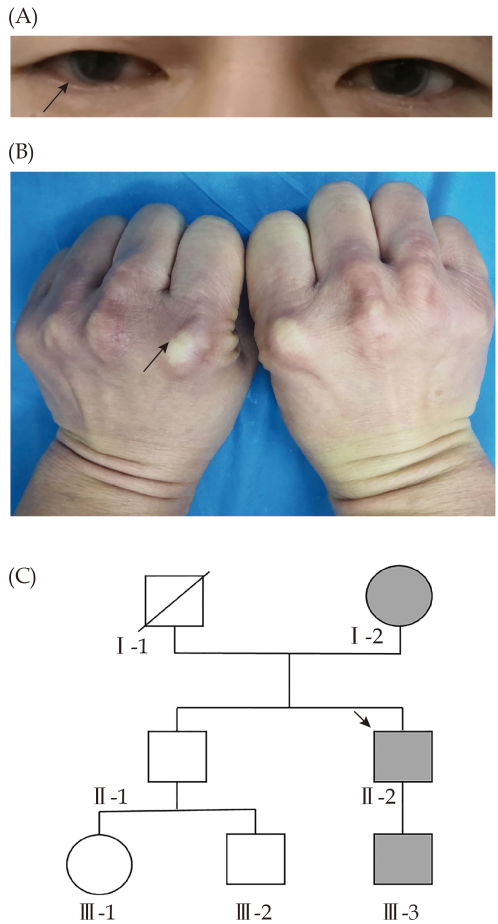

Figure 1 Clinical manifestation of the proband.

The blood lipids of the proband's father (I-1) were also elevated during his lifetime and slightly higher than his mother's (I-2). His older brother (II-1) also had elevated blood lipids. Furthermore, the cholesterol of his son (III-3) was higher than normal when he was 11 years old. The detailed family pedigree chart is presented in Figure 1C. Specifically, the total cholesterol, LDL-C, and Apo B in the proband (II-2) and his mother (I-2) were higher than those of the other members, while the HDL-C and Apo A levels were lower. In addition, TC, LDL-C, and Apo B levels of I-1 were increased. Besides, TG levels in III-3 were the highest (Table 1). Therefore, the family was diagnosed with FH.

Variant Detection

Next, we detected all variants, and a total of 143,228 variants covering 125,773 SNPs and 17,455 InDels were identified using WES. Among them, there were 749 new SNPs and 1481 new InDels. A summary of the WES data is presented in Supplementary Table 1. The selection of the variant (Table 2 and Table 3) was based on the combination of bioinformatics and the pathogenicity results reported in the literature about FH. When the frequency of variation was greater than 0.005 (public databases include KG, ESP, ExAC) and meaningless variants were excluded.

Then, a rare variant deleterious on *LDLR* gene was identified in the proband in chromosome19, position 11230801, c. 1879G > A, NM_000527, p.Ala627Thr, namely, rs879255066. This variant causes the alanine at position 627 to be changed to threonine, which is known to be a deleterious variant.[22] Combined with previous reports, we verified again that the *LDLR* c.1879G > A variant is a pathogenic variant.

Subsequently, sanger sequencing was performed to further validate the presence of the *LDLR* variant (c.1879G > A, p.Ala627Thr) in the proband. As shown in Figure 2, the proband (Ⅱ-2) carried the variant in *LDLR*.

Protein Structure Analysis

The variant (c.1879G > A, p.Ala627Thr) in *LDLR*

Table 1 Physical and laboratory examination.

Subjects	I-1	I-2	II-1	II-2	III-3
Gender	M	F	M	M	M
TG (< 1.7 mmol/L)	0.59	0.94	1.51	1.64	3.7
TC (< 5.18 mmol/L)	8.6	10.2	5.8	8.47	6.32
HDL-C (> 1.04 mmol/L)	1.49	1.04	0.89	0.77	1.75
LDL-C (< 3.37 mmol/L)	3.9	6.2	4.23	6.23	3.72
ApoA (1.22-1.61 g/L)	1.44	1.23	-	1.00	-
ApoB (0.69-1.05 g/L)	1.74	3.58	-	1.81	-

Apo A: apolipoprotein A; Apo B: apolipoprotein B; F: female; HDL-C: high density lipoprotein cholesterol; LDL-C: low density lipoprotein cholesterol; M: male;TC: total cholesterol; TG: triglyceride.

Table 2 Pathogenicity results of candidate gene mutation sites predicted by bioinformatics.

GENE	HGVSc	SIFT	PolyPhen2_HDIV	PolyPhen2_HVAR	MutationTaster	MutationAssessor	FATHMM	GERP_plus
LDLR	c.1879G > A	0.001	0.972	0.939	1	2.05	-4.55	5.37

HGVSc: human genome variation society cDNA; SIFT: Deleterious (< 0.05); PolyPhen2_HDIV: Probably damaging (≥ 0.957), possibly damaging (0.453 ≤ pp2_hdiv ≤ 0.956); benign (≤ 0.452); PolyPhen2_HVAR: Probably damaging (≥ 0.909), possibly damaging (0.447 ≤ pp2_hdiv ≤ 0.909); benign (<=0.446); MutationTaster: Deleterious(> 0.5); MutationAssessor: Deleterious(> 1.938); FATHMM: Deleterious(< -1.5); GERP_plus: Deleterious(> 3).

Table 3 Information of candidate pathogenic gene loci.

CHR	POS	ID	REF	ALT	GENE	HGVSc	HGVSp
19	11230801	rs879255066	G	A	*LDLR*	c.1879G>A	p.Ala627Thr

ALT: alternative; CHR: chromosome; HGVSc: human genome variation society; HGVSp: human genome variation society protein; ID: identification; POS: position; REF: Reference.

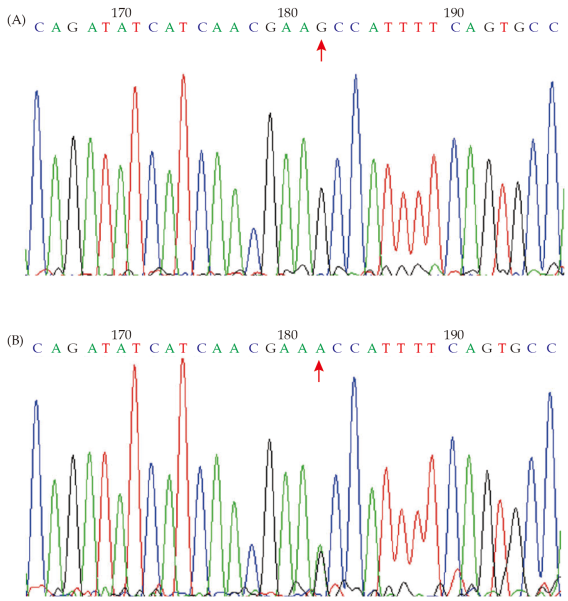

Figure 2 Sequencing data of *LDLR* loci. The arrow indicates corneal arcus (A), and skin xanthoma of the proband (B). Pedigree chart of the family. The arrow indicates the proband (II-2). Affected members are shown by the gray shades, the deceased member is indicated by symbol with a slash (C). LDLR: low-density lipoprotein receptor.

is a deleterious variant. When the non-polar alanine at position 627 in the peptide chain (Figure 3A) is mutated into a polar threonine (Figure 3B), the secondary structure of proteins is altered. Hydrogen bond formation was increased in variant proteins, which resulted in an increase in hydrophilicity, and transformation of several amino acids from planar to tetrahedral, which will affect LDL binding, the dissociation of ligand and receptor, and also receptor recycling. In addition, we analyzed the *LDLR* gene of several species and found that the alanine at position 627 is highly conserved (Table 4).

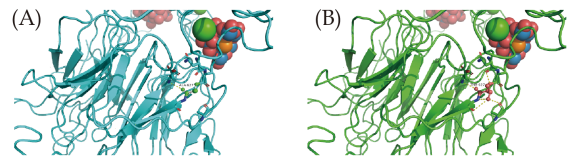

Figure 3 Changes in protein spatial structure. (A): The wild genotype of *LDLR* is listed, and the variant genotype corresponding to it is listed below (B). LDLR: low-density lipoprotein receptor. The normal protein structure of LDLR is listed on the left (A), and the variant protein corresponding to it is listed on the right (B). The yellow dotted line represents the hydrogen bond. LDLR: low-density lipoprotein receptor.

LDLR Variant Induced NLRP3-Dependent Pyroptosis in L02 Cells

To reveal the underlying mechanism of *LDLR* variant induced hypercholesterolemia, we detected the change in LDL uptake caused by the *LDLR* variant. As shown in Figure 4A & B, the results showed that the expression of wild-type or variant LDLR was significantly higher than the control group. LDL is internalized by endocytosis after binding to the LDLR. Following that, we used confocal imaging to detect LDL uptake. As shown by the enhanced fluorescence intensity in Figure 4C & D, we found increased uptake of LDL in the variant group. Additionally, our results from cholesterol measurement assaying showed that, compared with the control or wild type group, the intracellular cholesterol level was obviously higher in the variant group (Figure 4E). Importantly, cholesterol crystals have been shown to cause NLRP3 inflammasome activation, which is closely related to pyroptosis.[19,24] Our results indicated that, compared with the control or wild-type group, the expression of pyroptosis-related genes, including NLRP3, ASC, C-caspase1, GSDMD, IL-18,

Table 4 Evolutionary conservation analysis for the p.Ala627Thr mutation in *LDLR*.

Protein Acc.	Gene	Organism		Amino acid sequences	
NP_000518.1	*LDLR*	H.sapiens	596	KTILEDEKRLAHPFSLAVFEDKVFWTDIINE**A**IFSANRLTGSDVNLLAEN	645
XP_001167447.1	*LDLR*	P.troglodytes	596	KTVLEDEKRLAHPFSLAVFEDKVFWTDIINE**A**IFSANRLTGSDVNLLAEN	645
NP_001028078.1	*LDLR*	M.mulatta	589	KTILEDKERLAHPFSLAIFEDKVFWTDIINE**A**IFSANRLTGSDINLLAEN	638
XP_005632926.1	*LDLR*	C.lupusfamiliaris	598	KTILEDKKKLAHPFSLAIFEDKIFWTDIINE**A**IFSANRLTGSDINLVAEN	647
NP_001160002.1	*LDLR*	B.taurus	598	KTVLEDKKKLAHPFSLAIFED KVFWTDVINE**A**IFSANRLTGSDISLMAEN	647
NP_034830.2	*LDLR*	M.musculus	596	KTILEDENRLAHPFSLAIYEDKVYWTDVINE**A**IFSANRLTGSDVNLVAEN	645
NP_786938.1	*LDLR*	R.norvegicus	596	KTILEDEKQLAHPFSLAIYEDKVYWTDVLNE**A**IFSANRLTGSDVNLVAKN	645
NP_001025454.1	*LDLR*	D.rerio	552	RTLIIDQGKLAHPLSLTVFEEKVFWTDVSNNA**A**ILSANRVTGGDITKVAEH	601
XP_002942891.1	*LDLR*	X.tropicalis	596	ITVISDETHLAHPFGLTVFED LVFWTDIENE**A**IFSANRLTGSNIT KVA ED	645

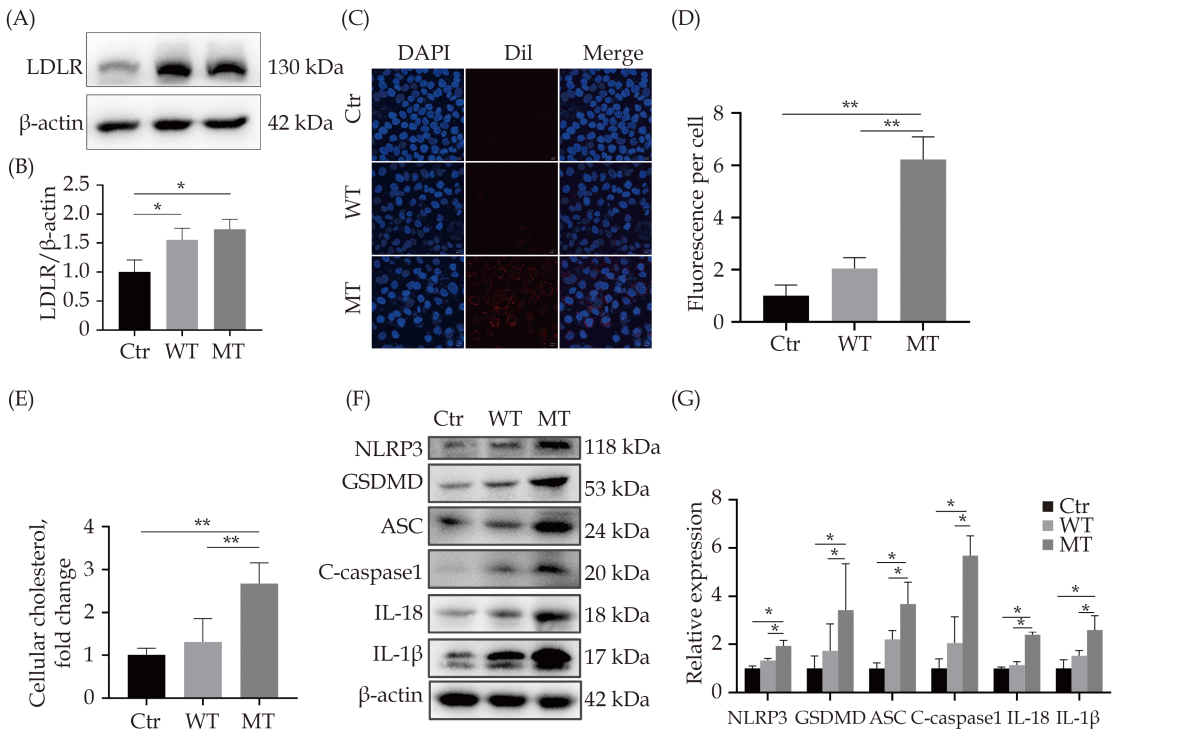

Figure 4 *LDLR* variant was related to NLRP3-induced pyroptosis in L02 cells. (A & B): The overexpression efficiency of LDLR was evaluated at the protein level, $^{*}P < 0.05$; (C & D): the internalization of DiI-LDL was detected by confocal microscope, $^{**}P < 0.01$; (E) Intracellular cholesterol levels were detected after transfection of overexpression plasmids; (F & G): after overexpression of wild-type or variant *LDLR* 48h, LDL (200 μg/mL) was incubated with indicated groups for 24h and the expression of pyroptosis related genes was detected; $^{*}P < 0.05$. Ctr: control; LDLR: low-density lipoprotein receptor; MT: mutation type; WT: wild type.

IL-1β, was significantly elevated in the variant group (Figure 4F & G).

ROS was Participated in NLRP3-Mediated Pyroptosis in L02 Cells

Cellular ROS exerts a crucial role on NLRP3 inflammasome activation. To further confirm the role of ROS in pyroptosis after the *LDLR* variant, we conducted a ROS inhibition study by using the ROS inhibitor NAC. In contrast to the control or wild-type group, intracellular ROS levels were significantly elevated in the *LDLR* variant group, which were significantly reduced treated with NAC (Figure 5A). To evaluate the effect of ROS on pyroptosis after the *LDLR* variant, we detected the expression of pyroptotic molecules and found suppressed expression of NLRP3, ASC, C-caspase1, GSDMD, IL-18, IL-1β after NAC treatment (Figure 5B, C). Besides, the pyroptosis induced by the *LDLR* variant was alleviated after the inhibition of ROS with NAC (Figure 5D, E).

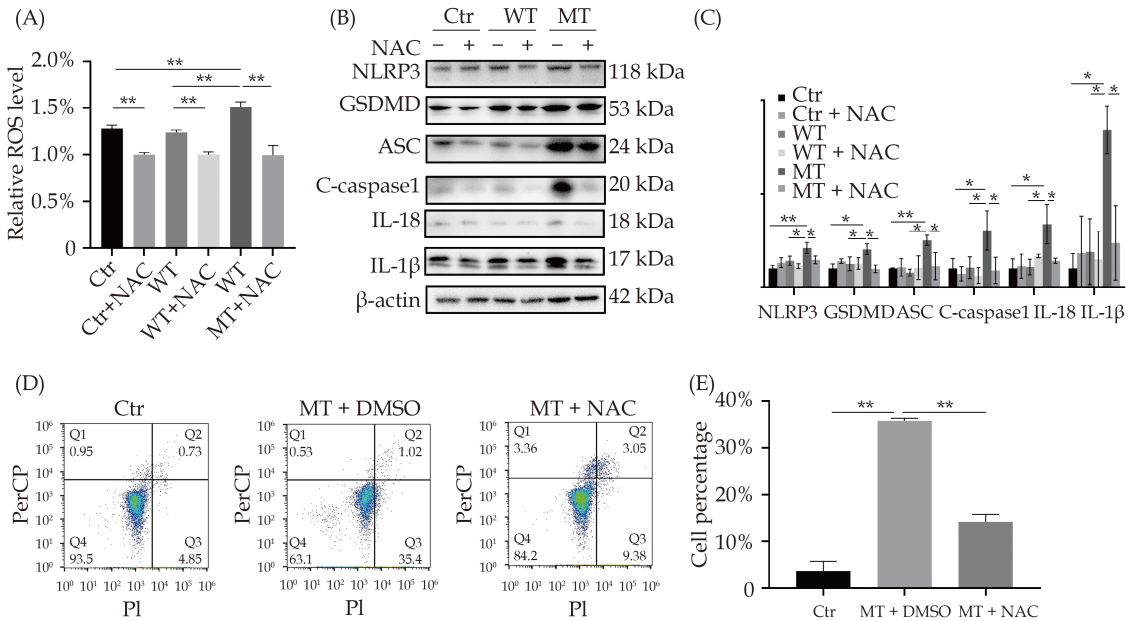

Figure 5 ROS participated in NLRP3-mediated pyroptosis in L02 cells. (A): After overexpression of wild-type or variant *LDLR* 48h, LDL (200 μg/mL) was incubated with indicated groups for 24 h and the levle of ROS was detected, $^{*}P < 0.05$; $^{**}P < 0.01$; (B & C): after overexpression of wild type or variant *LDLR* 48 h, cells were preincubated with NAC, LDL (200 μg/mL) and the expression of pyroptosis related genes was detected; $^{*}P < 0.05$; $^{**}P < 0.01$; (D & E): flow cytometry was applied to detect the pyroptosis in indicated groups; $^{**}P < 0.01$. Ctr: control; LDLR: low-density lipoprotein receptor; MT: mutation type; NAC: N-acetyl-L-cysteine; ROS: reactive oxygen species; WT: wild type.

These data suggested that the LDL binds to the *LDLR* variant activates the NLRP3 inflammasome and pyroptosis by increasing ROS generation.

DISCUSSION

The global prevalence of FH is high, but the number of confirmed cases is very low.[13,25] In addition, there is very little research on the FH gene variant in China compared to other countries; thus, little is known on the gene variant spectrum among Chinese patients.[5,6,26] However, FH should be diagnosed and treated early to prevent hypercholesterolemia from causing damage to other organs. Early diagnosis can be achieved through genetic testing, which can enable early treatment of FH patients.

In the present study, we identified the sequence variations of all genes in the proband diagnosed with FH using WES. A rare, deleterious heterozygous variant (LDLR: c. 1879G > A, NM_000527, p.Ala627Thr) in *LDLR* was associated with FH and was considered to be a pathogenic variant for FH. In addition, through this exploratory study, we found that this variant may lead to the accumulation of cholesterol and the production of ROS later, which resulted in NLRP3-dependent pyroptosis. Importantly, compared to the wild group, ROS levels were significantly higher in the variant group; the use of the ROS inhibitor NAC alleviated the increase in expression of LDL-induced NLRP3-mediated pyroptosis-related genes. This suggests that the failure of the *LDLR* variant to degrade intracellular LDL leads to an increase in intracellular cholesterol levels, which in turn promotes ROS production and hepatocyte pyroptosis. Hepatocytes are the main organ for LDL metabolism [15], and hepatocyte pyroptosis is one of the causes of FH due to *LDLR* variant.

Familial hypercholesterolemia is mainly caused by variants in the *LDLR* gene, accounting for 93% of all variants.[13,27] The LDL receptor expressed on the cell membrane regulates the plasma cholesterol level by identifying, binding, and internalizing the circulating LDL-C, eliminating the circulating LDL-C.[28] Low density lipoprotein receptor (LDLR) is encoded by the *LDLR* gene containing 18 exons and translated into 860 amino acids, located on Ch19p-13.113.3.[29,30] The variant occurs on the 13th exon changing the β-sheet and increasing the pH, which may decrease the recognition, binding, and endocytosis of LDL, subsequently forming a tight com-

plex between LDL and LDLR, which cannot be separated, resulting in hypercholesterolemia. Furthermore, the alanine at position 627 is located in the EGF precursor domain consisting of 400 amino acids, which facilitates the dissociation of the LDL particles from the LDLR-LDL complex in the endosome.[30] This may explain the higher content of cholesterol in the variant *LDLR* group to a certain extent. Thus, when alanine mutates to threonine, LDL and LDLR may form tight complexes, eventually forming hypercholesterolemia.

Our findings are consistent with previous reports that the *LDLR* p.(Ala627Thr) variant is associated with FH.[29,31,32] This variant had a frequency of 0.00000406 according to the GnomAD database and was classified as pathogenic in the ClinVar database. Our study confirmed that this variant is a pathogenic FH variant. In addition, the spectrum of variants among the Chinese people with FH has been expanded, making genetic diagnosis more accurate, on time, and treatments to be implemented accordingly.

Limitations

Our study should be interpreted within the context of its limitations. Firstly, the number of included pedigrees in this research was small and therefore the detection of pathogenic variants was limited. Secondly, in addition to testing lipid-related indicators, ROS levels and pyroptosis-related gene expression in this family should also be further tested. Finally, this work was only studied in cells and needs to be further validated by *in vivo* experiments.

Conclusions

In summary, the present study describes a missense variant in the *LDLR* gene in a Chinese family with FH, which will help the early diagnosis and treatment of FH patients. The pathogenic mechanism may be due to ROS/NLRP3 activation promoting pyroptosis after *LDLR* variant. This study contributes to the genotypic characterization of FH in China, which is relevant for genetic counseling, diagnosis, and treatments. Whole-exome sequencing is a quick, accurate, and reliable technique to identify gene variants in suspected FH patients.

DISCLOSURE

Authors' Contributions

Conceived and designed the experiments: SJ and JYL. Performed the experiments: XCW, JYL and APD. Analyzed the data: JYL, WZC, XD, CL and WHW. Wrote the paper: WZC and JYL. WZC and WHW contributed equally. All authors read and approved the final manuscript.

Acknowledgments

This study was supported by the Health and Family Planning Commission of Wuhan City (Grant Number WX18M02) and Central Guiding Local Science and Technology Development Special Project (No. 2022BGE272). The authors thank all the volunteers that participated in this study. All authors had no conflicts of interest to disclose.

REFERENCES

[1] Amersfoort J, Schaftenaar FH, Douna H, *et al*. Diet-induced dyslipidemia induces metabolic and migratory adaptations in regulatory T cells. *Cardiovasc Res* 2021; 117: 1309–1324.
[2] Foody JM, Vishwanath R. Familial hypercholesterolemia/autosomal dominant hypercholesterolemia: Molecular defects, the LDL-C continuum, and gradients of phenotypic severity. *J Clin Lipidol* 2016; 10: 970–986.
[3] Abifadel M, Varret M, Rabès JP, *et al*. Mutations in PCSK9 cause autosomal dominant hypercholesterolemia. *Nat Gene* 2003; 34: 154–156.
[4] Alnouri F, Athar M, Al-Allaf FA, *et al*. Novel combined variants of LDLR and LDLRAP1 genes causing severe familial hypercholesterolemia. *Atherosclerosis* 2018; 277: 425–433.
[5] Pirillo A, Garlaschelli K, Arca M, *et al*. Spectrum of mutations in Italian patients with familial hypercholesterolemia: New results from the LIPIGEN study. *Atheroscler Suppl* 2017; 29: 17–24.
[6] Danyel M, Ott CE, Grenkowitz T, *et al*. Evaluation of the role of STAP1 in Familial Hypercholesterolemia. *Sci Rep* 2019; 9: 11995.
[7] Cao YX, Wu NQ, Sun D, *et al*. Application of expanded genetic analysis in the diagnosis of familial hypercholesterolemia in patients with very early-onset coronary artery disease. *J Transl Med* 2018; 16: 345.
[8] de Paiva Silvino JP, Jannes CE, Tada MT, *et al*. Cascade screening and genetic diagnosis of familial hypercholesterolemia in clusters of the Southeastern region from Brazil. *Mol Biol Rep* 2020; 47: 9279–9288.
[9] Bandyopadhyay D, Ashish K, Hajra A, *et al*. Cardiovascular Outcomes of PCSK9 Inhibitors: With Special Emphasis on Its Effect beyond LDL-Cholesterol Lowering. *J Lipids* 2018; 2018: 3179201.

[10] Flannick J, Mercader JM, Fuchsberger C, *et al*. Exome sequencing of 20, 791 cases of type 2 diabetes and 24, 440 controls. *Nature* 2019; 570: 71–76.
[11] Jelin AC, Vora N. Whole Exome Sequencing: Applications in Prenatal Genetics. *Obstet Gynecol Clin North Am* 2018; 45: 69–81.
[12] Hansen MC, Haferlach T, Nyvold CG. A decade with whole exome sequencing in haematology. *Br J Haematol* 2020; 188: 367–382.
[13] Xiang R, Fan LL, Lin MJ, *et al*. The genetic spectrum of familial hypercholesterolemia in the central south region of China. *Atherosclerosis* 2017; 258: 84–88.
[14] van den Boomen DJH, Sienkiewicz A, Berlin I, *et al*. A trimeric Rab7 GEF controls NPC1-dependent lysosomal cholesterol export. *Nat Commun* 2020; 11: 5559–5559.
[15] Ochiai A, Miyata S, Shimizu M, *et al*. Piperine induces hepatic low-density lipoprotein receptor expression through proteolytic activation of sterol regulatory element-binding proteins. *PloS one* 2015; 10: e0139799.
[16] Bjune K, Wierød L, Naderi S. Inhibitors of AKT kinase increase LDL receptor mRNA expression by two different mechanisms. *PloS one* 2019; 14: e0218537–e0218537.
[17] Ho CM, Ho SL, Jeng YM, *et al*. Accumulation of free cholesterol and oxidized low-density lipoprotein is associated with portal inflammation and fibrosis in nonalcoholic fatty liver disease. *J Inflamm (Lond)* 2019; 16: 7.
[18] Burillo-Sanz S, Montes-Cano MA, García-Lozano JR, *et al*. Mutational profile of rare variants in inflammasome-related genes in Behçet disease: A Next Generation Sequencing approach. *Sci Rep* 2017; 7: 8453–8453.
[19] Qiu T, Pei P, Yao X, *et al*. Taurine attenuates arsenic-induced pyroptosis and nonalcoholic steatohepatitis by inhibiting the autophagic-inflammasomal pathway. *Cell Death Dis* 2018; 9: 946–946.
[20] Risk of fatal coronary heart disease in familial hypercholesterolaemia. Scientific Steering Committee on behalf of the Simon Broome Register Group. *BMJ (Clinical research ed)* 1991; 303: 893–896.
[21] Iacovazzo D, Flanagan SE, Walker E, *et al*. MAFA missense mutation causes familial insulinomatosis and diabetes mellitus. *Proc Natl Acad Sci U S A* 2018; 115: 1027–1032.
[22] Pace NP, Craus J, Felice A, Vassallo J. Case Report: Identification of an HNF1B p. Arg527Gln mutation in a Maltese patient with atypical early onset diabetes and diabetic nephropathy. *BMC Endocr Disord* 2018; 18: 28.
[23] Sunyaev S, Ramensky V, Bork P. Towards a structural basis of human non-synonymous single nucleotide polymorphisms. *Trends Genet* 2000; 16: 198–200.
[24] Grebe A, Latz E. Cholesterol crystals and inflammation. *Curr Rheumatol Rep* 2013; 15: 313.
[25] Sun LY, Zhang YB, Jiang L, *et al*. Identification of the gene defect responsible for severe hypercholesterolaemia using whole-exome sequencing. *Sci Rep* 2015; 5: 11380.
[26] Brunham LR, Ruel I, Aljenedil S, *et al*. Canadian cardiovascular society position statement on familial hypercholesterolemia: update 2018. *Can J Cardiol* 2018; 34: 1553–1563.
[27] Cayo MA, Mallanna SK, Di Furio F, *et al*. A drug screen using human ipsc-derived hepatocyte-like cells reveals cardiac glycosides as a potential treatment for hypercholesterolemia. *Cell Stem Cell* 2017; 20: 478–489.e475.
[28] van de Sluis B, Wijers M, Herz J. News on the molecular regulation and function of hepatic low-density lipoprotein receptor and LDLR-related protein 1. *Curr Opin Lipidol* 2017; 28: 241–247.
[29] Cheng X, Ding J, Zheng F, *et al*. Two mutations in LDLR gene were found in two Chinese families with familial hypercholesterolemia. *Mol Biol Rep* 2009; 36: 2053–2057.
[30] Oommen D, Kizhakkedath P, Jawabri AA, *et al*. Proteostasis regulation in the endoplasmic reticulum: an emerging theme in the molecular pathology and therapeutic management of familial hypercholesterolemia. *Front Genet* 2020; 11: 570355.
[31] Sun XM, Patel DD, Webb JC, *et al*. Familial hypercholesterolemia in China. Identification of mutations in the LDL-receptor gene that result in a receptor-negative phenotype. *Arterioscler Thromb* 1994; 14: 85–94.
[32] Jiang L, Sun LY, Dai YF, *et al*. The distribution and characteristics of LDL receptor mutations in China: A systematic review. *Sci Rep* 2015; 5: 17272.

Please cite this article as: CHENG WZ, WANG WH, DENG AP, DANG X, LIU C, WANG XC, LI JY, JIN S. Identification of an *LDLR* variant in a Chinese familial hypercholesterolemia and its relation to ROS/NLRP3-Mediated pyroptosis in hepatic cells. *J Geriatr Cardiol* 2023; 20(5): 341–349. DOI: 10.26599/1671-5411.2023.05.003